Enhancement to Luminescent Efficiencies by Thermal Rearrangement from *ortho*- to *meta*-Carborane in Bis-Carborane-Substituted Acenes

Hirofumi Naito[1], Kyoya Uemura[1], Yasuhiro Morisaki[1,2], Kazuo Tanaka[1]*, and Yoshiki Chujo[1]*

[1]*Department of Polymer Chemistry, Graduate School of Engineering, Kyoto University, Katsura, Nishikyo-ku, Kyoto 615-8510, Japan*

[2]*Present address: Department of Applied Chemistry for Environment, School of Science and Technology, Kwansei Gakuin University, 2-1 Gakuen, Sanda, Hyogo 669-1337, Japan*

E-mail: tanaka@poly.synchem.kyoto-u.ac.jp (K.T.); chujo@poly.synchem.kyoto-u.ac.jp (Y.C.)

HP: http://poly.synchem.kyoto-u.ac.jp/

Abstract

In the previous study, we synthesized the series of bis-*o*-carborane-modified acenes and revealed various unique luminescent behaviors such as highly-efficient solid-state emission and luminochromism. In this manuscript, we report further enhancements of the bis-*o*-carborane-modified acenes to luminescent efficiencies by thermally-induced structural rearrangement from *ortho*- to *meta*-carborane. We found the thermal rearrangements of the anthracene derivative **1** can occur near the melting points and obtained the luminescent products. From the detailed investigation with the product from **1**, transformation of the molecular structure was proved by X-ray crystallography. In addition, it was indicated that rearrangement occurred at only one of two *o*-carborane units by heating at 300 °C. According to theoretical investigations with **1** for transition states with quantum calculation, it was proposed that thermal rearrangement could proceed because of low activation energy in the first rearrangement step by the connection with anthracene. From optical measurements, enhancements of not only luminescent efficiencies but also aggregation-induced emission enhancement were observed. Furthermore, it was demonstrated that this strategy for enhancing emission properties was applicable with the tetracene molecule to obtain the deep-red luminescent dye.

Introduction

To obtain functional organic materials, one of promising strategies is to utilize an "element-block", which is defined as a minimum functional unit composed of heteroatoms.[1] For example, by connecting luminescent boron "element-blocks" with an environment-sensitive unit, various types of stimuli-responsive materials were readily constructed according to preprogrammed designs. Based on this strategy, *o*-carborane is recognized as a versatile "element-block" especially for designing solid-state luminescent materials with chromic properties.[2–4] Carborane ($C_2B_{10}H_{12}$) is an icosahedral cluster compounds consisting of 10 boron atoms and 2 carbon atoms.[5–10] Based on their unique features such as the rich boron content and high thermal and chemical stability, the applications of carboranes for use in the fields of medicinal chemistry and material science have been extensively studied.[5–10]

More recently, *o*-carborane has attracted attention as a key unit for optically-functional materials.[11–38] *o*-Carborane is known to work as an electron-acceptor because of nature of electron-deficient three-center-two-electron bonds when bonded with the electron-donor at the carbon,[39,40] and bright emission from the induced charge transfer (ICT) state can be obtained by combination with electron-donating units.[41] It should be mentioned that bright emission from this ICT state was often observed even in the solid state by suppressing aggregation-caused quenching (ACQ).[42–46] Moreover, emission enhancements by solidification were detected.[42–48] Additionally, it was found that some of solid-state emissive *o*-carborane derivatives showed luminescent chromic behaviors toward external stimuli such as heating, vapor fuming, and scratching[47] From the series of mechanical studies, it has been proposed that intramolecular vibration at the C−C bond

in the *o*-carborane unit and rotation at the connecting bond should be responsible for presenting emission enhancements in the condensed state and luminescent chromism, respectively.

Herein, we synthesized the bis-*o*-carborane-modified acenes [48,49] and observed enhancements of luminescent properties by thermally-induced unique structural transformation from *o*- to *m*-carborane, which is a structural isomer of *o*-carborane and possesses two carbon atoms on the 1,7-position. Initially, by heating the anthracene derivative **1** up to 300 °C, the irreversible luminescent color change was detected, and the luminescent product was successfully isolated. It was revealed from the X-ray single crystal analysis that one of two *o*-carborane units rearranged to *m*-carborane **2** (Scheme 1). According to theoretical investigation, it was suggested that transformation could proceed owing to lowering effect of the anthracene moiety on the energy barrier in the transition. Furthermore, it was demonstrated that the isomerization can improve emission efficiencies both in solution and solid states. Finally, we also observed that this strategy was applicable in the deep-red luminescent molecule composed of tetracene instead of anthracene. So far, *m*-carboranes were often simply used as an electron-accepting unit in ACQ-presenting commodity luminescent dyes. In this study, it is demonstrated that the thermal rearrangement to *m*-carborane can be a facile strategy for enhancing luminescent property.

Scheme 1

Results and Discussion

It was reported that some *m*-carborane derivatives were generated via thermal rearrangements of *o*-carborane.[5,50–53] By heating above 425 °C, *o*-carborane transformed to more stable *m*-carborane irreversibly. Since the discovery of *o*-carborane and its thermal rearrangement to *m*-carborane, many researchers have studied its mechanism experimentally and theoretically.[5,50–53] Recently, computational analyses were performed by M. L. Mckee and co-workers.[52] Accordingly, it was proposed that the rearrangement proceeds via a triangular-face rotation (TFR) process (Scheme 1). Highly-thermal stability of the carborane boron–aryl carbon bond was suggested in the gas-phase rearrangement of 3-aryl-*o*-carborane at 550−600 °C to 2- and 4-aryl-*m*-carboranes under vacuum.[54] In C,C'-bis-substituted *o*-carboranes having bulky groups, cage rearrangement occurred at lower temperature. Bond cleavages could be assisted by steric repulsion between the substituents. For example, 1,2-$(RPh_2Si)_2C_2B_{10}H_{10}$ (R = Me, Cl) and 1,2-$(ClMe_2Si)_2C_2B_{10}H_{10}$ presented isomerization to the corresponding *m*-carborane derivatives at 260 and 280 °C, respectively.[55,56] In contrast, bond cleavage at aryl-C(cage) was initiated in 1-phenyl-*o*-carborane at 300 °C.[57] Thus, in general, thermal rearrangements of 1- and/or 2-aryl-*o*-carborane hardly proceeded.

Taking account of potential isomerization of *o*-carborane, we also investigated thermal reactivity of the bis-*o*-carborane-modified acenes. Syntheses were performed according to the previous reports,[48,49] and initially the red-luminescent crystal of the anthracene derivative **1** involving $CHCl_3$ as a crystalline solvent was prepared. The powder sample of **1**·$CHCl_3$ was heated at 300 °C for 10 min in the DSC apparatus, and thermal behaviors were monitored. Figure 1 shows the TGA and DSC profiles of **1**·$CHCl_3$ crystal under N_2

atmosphere. In the DSC profile, the endothermic peaks around 120 °C and at 272 °C were obtained attributable to the loss of solvent molecules and melting point, respectively. It should be noted that large exothermic peak was detected at 276 °C. In the TGA profile, the loss of mass occurred over 340 °C. This fact suggests that the exothermic reaction should proceed around the melting point of **1**. From the pan in the DSC apparatus, the products were analyzed with HPLC in chloroform and the significant single peak was detected (Chart S1). After collection, the orange product with almost same red-luminescent property was able to be isolated with HPLC. The resulting product **2** showed good stability and solubility in common organic solvents such as chloroform, dichloromethane and tetrahydrofuran. Thereby, conventional characterization methods in organic synthesis such as NMR spectroscopies and mass measurement were applicable (see Experimental Section and Charts S2−S4). Further analyses were performed with **2**.

Figure 1

^{1}H and ^{11}B NMR spectra of **1** and **2** were compared (Figures S1 and S2). It was indicated that the single chemical component was generated according to the ^{1}H NMR spectrum. The signal peaks corresponding to 1,4,7,8-positions of the anthracene moiety shifted from 8.60 ppm to 8.79 and 9.16 ppm completely, and broad peak derived from B-*H* hydrogens of the carborane cluster was detected. These data indicate that the exothermic reaction should be not pyrolysis but transformation with maintaining the carborane cluster. By heating over 320 °C, losses of signal peaks were observed, indicating that not the second rearrangement but decomposition occurred in the sample.

Molecular structure of **2** was confirmed by X-ray crystallography (Figure 2, Table S1). Single crystal of **2** suitable for X-ray crystallography was obtained by slow evaporation of the $CHCl_3$/MeOH solution containing **2**. Surprisingly, only one *o*-carborane moiety was rearranged to *m*-carborane. In the crystal structure of **2**, it was shown that the anthracene ring formed a π-stacked dimer with the neighboring anthracene, similarly to its precursor **1** (Figure S3).[49] The overlapping area of two π-stacked anthracenes was estimated as 16%, and the distance between the centers of each anthracene was 4.44 Å, which was much shorter than those in **1**·solvent. This is probably because the phenyl ring connected to the *m*-carborane moiety could be spatially far from the adjacent anthracene moiety followed by reducing steric repulsion between two molecules. From the comparison with the crystalline packings before and after the rearrangement,[49] it was proposed that the rearrangement could proceed at the phenyl ring which was isolated from the π-dimer of the central anthracenes because of less structural restriction by stacking. The ring strain of **2** was evaluated with ring deformation angles α and β toward the central ring. The α and β values for the ring of anthracene in **2** were 19.3° and 3.28°, respectively, which was similar to **1**·solvent (Table S2). Intermolecular π-π stacking between the anthracene rings and steric hindrances of the phenyl-substituted *o*-carboranes in the π-stacked dimer induced these large deformation angles just like the case of **1**·solvent. According to the ^{1}H NMR spectrum, another structural isomer, in which both *o*-carborane moieties rearranged to *m*-carboranes, was not detected. This fact implies that the activation energy in the second isomerization could be higher than that in the first one.

Figure 2

To theoretically investigate the rearrangement process, quantum calculations were performed (Figure 3). Transition state calculations were carried out according to the calculation procedure by McKee *et al.*[52] Target species were optimized at the B3LYP/6-31G(d) level of theory and frequency calculations were carried out at the same level to confirm whether they are at the stationary points. In addition, zero-point energies and entropies as well as thermal correction data were obtained. Then, single-point electronic energies were calculated at the B3LYP/6-311+G(2d,p) level. The enthalpies for the species at 298 K were applied to the enthalpy at 500 and 800 K, and these values were used to determine the absolute free energy at 298, 500, and 800 K. Initially, it was confirmed that the optimized structures showed good correspondence to those in the crystal packing. Therefore, calculation parameters were used in the further theoretical study. According to the TFR model, transition states were proposed, and energy levels of each transition structure were estimated.[52] As model reactions, transition behaviors with *o*-carborane (***o*-Cb**), 1-phenyl-*o*-carborane (**Ph-*o*-Cb**), 1-anthracenyl-*o*-carborane (**Ant-*o*-Cb**) and 1-anthracenyl-2-phenyl-*o*-carborane (**Ant-Ph-*o*-Cb**) were also surveyed with the same calculation method for assessing the substituent effects on the rearrangement process (Scheme S1, Figures S4 and S5, and Tables S3 and S4). The activation energies of *ortho* to *meta* transition process of ***o*-Cb** and **Ph-*o*-Cb** were estimated to be 203.0 and 203.5 kJ/mol, respectively, while those of **Ant-*o*-Cb** and **Ant-Ph-*o*-Cb** were 141.7 and 148.5 kJ/mol, respectively, indicating that introduction of the anthracene moiety decreased the activation energy. As shown in the previous experimental results, it is likely that steric repulsion could contribute to facilitating isomerization by lowering the activation energy.[49] It should be noted that this lowering effect on the activation energy should play a significant role in the rearrangement process. Calculations for the transition

states of **1** resulted in the rotation of the phenyl-*o*-carborane moiety as represented in **TS1**. Moreover, the successive *ortho* to *meta* rearrangement was observed in **TS2** with an activation energy of 103.0 kJ/mol, which is approximately the half energy in the isomerization of ***o*-Cb**. This significant low activation energy strongly suggests acceptance of the thermal rearrangement process before decomposition. Furthermore, the activation energy was estimated in the second *ortho* to *meta* isomerization (**TS3**), and consequently it was calculated to be 131.1 kJ/mol, which is higher than that in the first isomerization process. These data clearly indicate that the second rearrangement process should compete to the decomposition process because of high activation energy. Hence, the isomer having bis-*m*-carborane moieties was hardly obtained after heating.

Figure 3

The cyclic voltammograms (CV) were collected with **1** and **2** (Figure S6). Compound **1** showed two reduction peaks correspond to reduction to the dianion and then the tetraanion.[58−60] In contrast, **2** showed three distinct reduction peaks. The first two reduction peaks for **2** were the reductions to the monoanion radical and then the dianion. The third reduction in **2** should be lowered after the formation of the *m*-carborane cluster. The diaryl-*m*-carborane should be more difficult to be reduced than diaryl-*o*-carborane.[12] The first reduction potential of −0.64 V for **1** was remarkable because it was approximately by 0.5 V easier to be reduced than an identical bis carborane assembly to **1** but with a tetrafluorophenylene instead of the anthracenylene bridge.[58] The LUMO energy level was estimated from the peak onset potentials in the spectra, and the HOMO energy level was calculated from the LUMO energy level and the band gap energy

estimated from the absorption edge (Table S5). Both compounds showed remarkably low-lying LUMO energy levels of −4.16 eV and −4.13 eV for **1** and **2**, respectively. It is likely that introduction of two carborane moieties should be responsible for lowering energy levels of both frontier orbitals.

Influence on optical properties was examined in the rearrangement process. Figure 4a shows the UV−vis absorption and PL spectra of **1** and **2** in THF solution (1.0×10^{-5} M). Both absorption spectra exhibited the bands with the peaks around 280 nm and 450 nm attributable to typical π−π* transition in the phenyl and anthracene moieties, respectively, meanwhile distinct difference was observed in the PL spectra. Although both compounds presented emission bands from the ICT state at the similar positions around 650 nm, obvious increase in the emission intensity was observed from **2** (Table 1, Figure S7).[49] Notably, the absolute PL quantum efficiency (Φ_{PL}) of **2** was 0.19, which was much higher than that of **1** ($\Phi_{PL} < 0.01$). Additionally, aggregation-induced emission enhancement (AIEE) was clearly demonstrated from **2** in the aggregation (THF/H_2O = 1/99 (v/v), 1.0×10^{-5} M). Furthermore, **2** showed stronger emission in the crystalline state ($\Phi_{PL} = 0.59$). It was suggested in the previous reports that 1-anthracenyl-2-phenyl-*o*-carborane showed almost no emission in THF solution due to excitation deactivation via intramolecular vibration at the C−C bond in the *o*-carborane unit.[44] In the *meta*-form, these vibrational motions would be absent. As a result, emission enhancements were accomplished in solution by isomerization. In the aggregation, the *m*-carborane unit could play a critical role in suppression of ACQ, followed by emission enhancement without peak shift because of the steric hindrance. In the crystalline state, the stacking at the anthracene moiety was enhanced after thermal rearrangement according to the shorter distance in **2**

than that in **1**. Therefore, slight decrease in the emission efficiency and red shift of the emission band should be induced.

Figure 4 and Table 1

Finally, to evaluate applicability of thermal rearrangement-triggered emission enhancement, we performed the thermal treatments with the naphthalene and tetracene derivatives.[48] From the thermal measurements (Figures S8 and S9), the similar profile was obtained only from the tetracene derivative in DSC analyses, and the luminescent product was obtained. Based on this result, the several tens milligrams of the tetracene derivative was reacted and the product was analyzed. In summary, similarly to anthracene, emission efficiencies in both solution and solid states were detected after heating with the tetracene derivative (Tables 1 and S6, Figure S10). The pristine tetracene derivative showed slight emission in all states due to intermolecular interaction at the distant aromatic rings from the *o*-carborane units,[48,61−63] meanwhile significant emission efficiencies can be obtained after heating. In the solution state, the emission band was detected in the shorter wavelength region than that of the anthracene derivatives. This result proposed that the original emission from tetracene should be recovered by heating. As a result, the emission band was detected in the similar wavelength region to the pristine tetracene (450−650 nm). It was implied that the single *o*-carborane unit might play an insufficient role in excitation deactivation, resulting in emission enhancement after the thermal rearrangement. In the solid state before heating, emission bands in the longer wavelength region with small emission efficiencies were observed, indicating that intermolecular interaction, followed by ACQ occurred. After heating, blue-shifted

emission bands were observed in the aggregation and crystalline samples, proposing suppression of stacking. Disturbance to intermolecular interaction should be induced by *m*-carborane, followed by emission enhancement in the solid state. These data suggest two issues. Since thermal rearrangements occurred in relatively-wider acenes such as anthracene and tetracene, it is supported that electronic interaction between the *o*-carborane unit and the bridging acene moiety should play a positive role in reduction of energy barriers in the thermal reactions. Next, emission enhancement by the thermal rearrangement has applicability in the different molecule.

Conclusion

Unexpected emission enhancement by heating was observed from the bis-*o*-carborane-modified acenes. From the mechanistic study with the anthracene derivative, it was found that *ortho* to *meta* isomerization proceeded. X-ray crystallography revealed that one of two *o*-carborane units rearranged to *m*-carborane, and two molecules of **2** formed a π-stacked dimer in the crystal packing just like **1**. The thermal rearrangement process was simulated by quantum calculations, and two important issues were found. Firstly, introduction of the anthracene moiety can lower the activation energy in the rearrangement. Secondly, higher thermal assistance should be needed in the second isomerization at another *o*-carborane unit. Therefore, only one *o*-carborane moiety rearranged to *m*-carborane completely. Moreover, compound **2** showed enhanced luminescent properties both in solution and crystalline states, and the AIEE behavior was obtained. Finally, similar luminescent enhancement was also detected from the tetracene derivative. Aryl-modified carboranes are known to be a versatile platform for obtaining functional luminescent materials having highly-efficient solid-state emission and

luminescent chromic behaviors. This rearrangement reaction would contribute to extending the number of compounds in the material library. Thus, our findings could be useful for designing thermally-resistant solid-state emissive materials having multi-chromic characteristics based on *o*-carborane derivatives.

Experimental section

General. ^{1}H, ^{13}C, and ^{11}B NMR spectra were recorded on a JEOL JNM-EX400 instrument at 400, 100, and 128 MHz, respectively. The ^{1}H and ^{13}C chemical shift values were expressed relative to Me_4Si as an internal standard. The ^{11}B chemical shift values were expressed relative to $BF_3{\cdot}Et_2O$ as an external standard. High-resolution mass spectra (HRMS) were obtained on a Thermo Fisher Scientific EXACTIVE spectrometer for atmospheric pressure chemical ionization (APCI). Analytical thin-layer chromatography (TLC) was performed with silica gel 60 Merck F254 plates. Column chromatography was performed with Wakogel C-300 silica gel. UV−vis absorption spectra were obtained on a SHIMADZU UV3600 spectrophotometer. Photoluminescence (PL) spectra were obtained on a Horiba FluoroMax-4 luminescence spectrometer; absolute PL quantum efficiencies (Φ_{PL}) were determined using a Horiba FL-3018 Integrating Sphere. Differential scanning calorimetry (DSC) thermograms were recorded on a Seiko DSC200 instrument using approximately 1.5 mg of samples at heating rate of 10 °C / min under N_2 atmosphere. Thermogravimetric analysis (TGA) was carried out on a Seiko EXSTAR 6000 instrument at heating rate of 10 °C / min under N_2 atmosphere. Cyclic voltammetry (CV) was carried out on a BAS CV-50W electrochemical analyzer in DMF containing 0.1 M of sample and 0.1 M of Bu_4NClO_4 with a glassy carbon working electrode, a Pt counter electrode, a Ag/AgCl (Ag/Ag^+) reference electrode, and a ferrocene/ferrocenium

external reference. Recyclable preparative high-performance liquid chromatography (HPLC) was performed on a Japan Analytical Industry LC-918R (JAIGEL-1HH and 2HH columns) using $CHCl_3$ as an eluent (flow rate: 7.5 mL/min)

Synthesis.

Neat condition under N_2 atmosphere

1·$CHCl_3$ (3.6 mg, 4.9 μmol) was heated to 300 °C for 10 min under N_2 atmosphere by using DSC apparatus to obtain **2** (2.2 mg, 3.6 μmol, 73%). Further purification for optical measurements was carried out by using HPLC ($CHCl_3$ as an eluent). Single crystal of **2** suitable for X-ray crystallography was obtained by slow evaporation in the $CHCl_3$/MeOH solution. ^{1}H NMR (400 MHz, CD_2Cl_2): δ(ppm) 9.16 (2H, d, J = 9.0 Hz, Ar-*H*), 8.79 (2H, d, J = 9.0 Hz, Ar-*H*), 7.43 (2H, t, J = 7.3 Hz, Ar-*H*), 7.29 (7H, tt, J = 8.8 Hz, J = 3.3 Hz, Ar-*H*), 6.85 (2H, t, J = 4.0 Hz, Ar-*H*), 6.74 (3H, d, J = 7.3 Hz, Ar-*H*), 4.39−1.65 (20H, br, B-*H*). ^{13}C NMR (100 MHz, CD_2Cl_2): δ(ppm) 135.4, 134.9, 131.9, 131.6, 131.4, 131.2, 130.7, 129.4, 128.7, 128.6, 128.3, 126.0, 125.7, 125.1, 124.1, 122.3, 96.4, 90.8, 77.7, 77.6. ^{11}B NMR (128 MHz, CD_2Cl_2): δ(ppm) 1.1, 0.1, –2.3, –3.3, –9.3, –10.2. HRMS (APCI): Calcd. for $C_{30}H_{38}B_{20}$ $[M+H]^+$ m/z 619.4977, found m/z 619.4970.

Neat condition under air atmosphere

Crystals of **1**·$CHCl_3$ (3.2 mg, 4.4 μmol) was put between two glass slides and heated to 290 °C for 5 min under air atmosphere by using hot plate. After cooling, further purification was carried out by using HPLC ($CHCl_3$ as an eluent) to obtain **2** (1.8 mg, 2.9 μmol, 66%).

Solution condition

1·$CHCl_3$ (11.8 mg, 16 μmol) was dissolved in squalane (3 mL) and heated to 290 °C for 2 h under Ar atmosphere with stirring. After cooling, squalane was removed by silica gel column chromatography with hexane as an eluent and compound **2** was obtained (4.9 mg, 8.0 μmol, 50%).

Calculation method.

Transition state calculations were carried out by Gaussian 09 suit program[1], using the calculation procedure by McKee *et al.*[2] Target species were optimized at the B3LYP/6-31G(d) level of theory and frequency calculations were carried out at the same level to confirm whether they are at the stationary points. In addition, zero-point energies and entropies as well as thermal correction data were obtained. Then, single-point electronic energies were calculated at the B3LYP/6-311+G(2d,p) level. The enthalpies for the species at 298 K were applied to the enthalpy at 500 and 800 K, and these values were used to determine the absolute free energy at 298, 500, and 800 K.

ACKNOWLEDGMENT

This work was partially supported by the Konica Minolta Science and Technology Foundation (for K.T.) and a Grant-in-Aid for Scientific Research on Innovative Areas "New Polymeric Materials Based on Element-Blocks (No.2401)" (JSPS KAKENHI Grant Number JP24102013).

CCDC number of **2**: 1561095

References

1. Y. Chujo, K. Tanaka, *Bull. Chem. Soc. Jpn*. **2015**, *88*, 633−643.

2. K. Nishino, K. Hashimoto, K. Tanaka, Y. Morisaki, Y. Chujo, *Tetrahedron Lett.* **2016**, *57*, 2025−2028.

3. Y. Morisaki, M. Tominaga, T. Ochiai, Y. Chujo, *Chem. −Asian J.* **2014**, *9*, 1247−1251.

4. K. Nishino, Y. Morisaki, K. Tanaka, Y. Chujo, *New J. Chem.* **2017**, *15*, 10550−10554.

5. "Icosahedral carboranes: 1,2-$C_2B_{10}H_{12}$", In *Carboranes, 2nd Ed.*, R. N. Grimes, Academic Press: New York, 1970.

6. V. I. Bregadze, *Chem. Rev.* **1992**, *92*, 209−223

7. A. González-Campo, E. J. Juárez-Pérez, C. Viñas, B. Boury, R. Sillanpää, R. Kivekäs, R. Núñez, *Macromolecules* **2008**, *41*, 8458−8466

8. F. Issa, M. Kassiou, L. M. Rendina, *Chem. Rev.* **2011**, *111*, 5701−5722

9. G. Li, S. Azuma, S. Sato, H. Minegishi, H. Nakamura, *Bioorg. Med. Chem. Lett*. **2015**, *25*, 2624−2628

10. G. Li, S. Azuma, S. Sato, H. Minegishi, H. Nakamura, *J. Organomet. Chem*. **2015**, *798*, 189−195.

11. R. Núñez, M. Tarrés, A. Ferrer-Ugalde, F. F. d. Biani, F. Teixidor, *Chem. Rev*. **2016**, *116*, 14307−14378.

12. L. Böhling, A. Brockhinke, J. Kahlert, L. Weber, R. A. Harder, D. S. Yufit, J. A. K. Howard, J. A. H. MacBride, M. A. Fox, *Eur. J. Inorg. Chem*. **2016**, 403−412.

13. L. Weber, J. Kahlert, R. Brockhinke, L. Böhling, A. Brockhinke, H.-G. Stammler, B. Neumann, R. A. Harder, M. A. Fox, *Chem. –Eur. J*. **2012**, *18*, 8347−8357.

14. L. Weber, J. Kahlert, R. Brockhinke, L. Böhling, J. Halama, A. Brockhinke, H.-G. Stammler, B. Neumann, C. Nervi, R. A. Harder, M. A. Fox, *Dalton Trans*. **2013**, *42*, 10982−10996.

15. J. Kahlert, L. Böhling, A. Brockhinke, H.-G. Stammler, B. Neumann, L. M. Rendina, P. J. Low, L. Weber, M. A. Fox, *Dalton* M. A. *Trans*. **2015**, *44*, 9766−9781.

16. Y.-J. Cho, S.-Y. Kim, M. Cho, W.-S. Han, H.-J. Son, D. W. Cho, S. O. Kang, *Phys. Chem. Chem. Phys*. **2016**, *19*, 9702−9708.

17. S.-Y. Kim, Y.-J. Cho, G. F. Jin, W.-S. Han, H.-J. Son, D. W. Cho, S. O. Kang, *Phys. Chem. Chem. Phys*. **2015**, *17*, 15679−15682.

18. K.-R. Wee, Y.-J. Cho, S. Jeong, S. Kwon, J.-D. Lee, I.-H. Suh, S. O. Kang, *J. Am. Chem. Soc*. **2012**, *134*, 17982−17990.

19. B. H. Choi, J. H. Lee, H. Hwang, K. M. Lee, M. H. Park, *Organometallics* **2016**, *35*, 1771−1777.

20. R. Furue, T. Nishimoto, I. S. Park, J. Lee, T. Yasuda, *Angew. Chem. Int. Ed*. **2016**, *55*, 7171–7175.

21. M. Uebe, A. Ito, Y. Kameoka, T. Sato, K. Tanaka, *Chem. Phys. Lett*. **2015**, *633*, 190−194.

22. Y. Kameoka, M. Uebe, A. Ito, T. Sato, K. Tanaka, *Chem. Phys. Lett*. **2014**, *615*, 44−49.

23. S. Inagi, K. Hosoi, T. Kubo, N. Shida, T. Fuchigami, *Electrochemistry* **2013**, *81*, 368−370.

24. Z. Wang, P. Jiang, T. Wang, G. J. Moxey, M. P. Cifuentes, C. Zhang, M. G. Humphrey, *Phys. Chem. Chem. Phys*. **2016**, *18*, 15719−15726.

25. J. J. Peterson, A. R. Davis, M. Were, E. B. Coughlin, K. R. Carter, *ACS Appl. Mater. Interfaces* **2011**, *3*, 1796−1799.

26. L. Zhu, W. Lv, S. Liu, H. Yan, Q. Zhao, W. Huang, *Chem. Commun*. **2013**, *49*, 10638−10640.

27. D. Tu, P. Leong, Z. Li, R. Hu, C. Shi, K. Y. Zhang, H. Yan, Q. Zhao, *Chem. Commun*. **2016**, *52*, 12494−12497.

28. W. Zhang, Y. Luo, Y. Xu, L. Tian, M. Li, R. He, W. Shen, *Dalton Trans*., **2015**, *44*, 18130−18137.

29. S. Mukherjee, P. Thilagar, *Chem. Commun*. **2016**, *52*, 1070−1093.

30. X. Li, H. Yan, Q. Zhao, *Chem. –Eur. J*. **2016**, *22*, 1888−1898.

31. J. Park, Y. H. Lee, J. Y. Ryu, J. Lee, M. H. Lee, *Dalton Trans*. **2016**, *45*, 5667−5675.

32. Y. H. Lee, J. Park, S.-J. Jo, M. Kim, J. Lee, S. U. Lee, M. H. Lee, *Chem. –Eur. J*. **2015**, *21* 2052−2061.

33. A. M. Prokhorov, T. Hofbeck, R. Czerwieniec, A. F. Suleymanova, D. N. Kozhevnikov, H. Yersin, *J. Am. Chem. Soc*. **2014**, *136*, 9637−9642.

34. N. Shin, S. Yu, J. H. Lee, H. Hwang, K. M. Lee, *Organometallics* **2017**, *36*, 1522−1529.

35. N. V. Nghia, J. Oh, J. Jung, M. H. Lee, *Organometallics* DOI: 10.1021/acs.organomet.7b00139.

36. J. J. Schwartz, A. M. Mendoza, N. Wattanatorn, Y. Zhao, V. T. Nguyen, A. M. Spokoyny, C. A. Mirkin, T. Baše, P. S. Weiss, *J. Am. Chem. Soc*. **2016**, *138*, 5957−5967.

37. K. O. Kirlikovali, J. C. Axtell, A. Gonzalez, A. C. Phung, S. I. Khan, A. M. Spokoyny, *Chem. Sci*. **2016**, *7*, 5132−5138.

38. A. M. Prokhorov, P. A. Slepukhin, V. L. Rusinov, V. N. Kalinin, D. N. Kozhevnikov, *Chem. Commun*. **2011**, *47*, 7713−7715.

39. A. M. Spokoyny, C. W. Machan, D. J. Clingerman, M. S. Rosen, M. J. Wiester, R. D. Kennedy, C. L. Stern, A. A. Sarjeant, C. A. Mirkin, *Nat. Chem*. **2011**, *3*, 590−596.

40. A. C. Serino, M. E. Anderson, L. M. A. Saleh, R. M. Dziedzic, H. Mills, L. K. Heidenreich, A. M. Spokoyny, P. S. Weiss, *ACS Appl. Mater. Interfaces* **2017**, *9*, 34592−34596.

41. K. Kokado, Y. Chujo, *J. Org. Chem.* **2010**, *76*, 316−319.

42. H. Naito, K. Nishino, Y. Morisaki, K. Tanaka, Y. Chujo, *Angew. Chem. Int. Ed.* **2017**, *56*, 254−259.

43. K. Nishino, H. Yamamoto, K. Tanaka, Y. Chujo, *Org. Lett*. **2016**, *18*, 4064−4067.

44. H. Naito, K. Nishino, Y. Morisaki, K. Tanaka, Y. Chujo, *J. Mater. Chem. C* **2017**, *4*, 10047−10054.

45. K. Nishino, K. Tanaka, Y. Chujo, *Molecules* **2017**, *22*, 2009−2018.

46. K. Tanaka, K. Nishino, S. Ito, H. Yamane, K. Suenaga, K. Hashimoto, Y. Chujo, *Faraday Discuss*. **2017**, *196*, 31−42.

47. K. Nishino, H. Yamamoto, K. Tanaka, Y. Chujo, *Asian. J. Org. Chem*. DOI: 10.1002/ajoc.201700390.

48. H. Naito, K. Nishino, Y. Morisaki, K. Tanaka, Y. Chujo, *Chem. –Asian J*. **2017**, *12*, 2134−2138.

49. H. Naito, Y. Morisaki, Y. Chujo, *Angew. Chem., Int. Ed.* **2015**, *54*, 5084−5087.

50. H. D., Kaesz, R., Bau, H. A., Beall, W. N., Lipscomb, V. I. Bregadze, *J. Am. Chem. Soc.* **1967**, *89*, 4218−4220.

51. H., Hart, W. N. Lipscomb, *J. Am. Chem. Soc.* **1969**, *91*, 771−772.

52. C. A., Brown, M. L. McKee, *J. Molec. Model.* **2006**, *12*, 653−664.

53. I. J., Sugden, D. F., Plant, R. G. Bell, *Chem. Commun.* **2013**, *49*, 975−977.

54. V. N., Kalinin, N. I., Kobel'kova, L. I. Zakharkin, *J. Organomet. Chem.* **1979**, *172*, 391−395.

55. V. N., Kalinin, B. A., Izmailov, A. A., Kazantsev, A. A.L. I. ; Zhdanov, Zakharkin, *Zh. Obshch. Khim.* **1984**, *54*, 1208−1209.

56. R. M., Salinger, C. L. Frye, *Inorg. Chem.* **1965**, *4*, 1815−1816.

57. L. I., Zakharkin, V. N., Kalinin, T. N., Balykova, P. N., Gribkova, V. V. Korshak, *J. Gen. Chem. USSR (Engl. Transl.)* **1973**, *43*, 2249−2254.

58. J. Kahlert, H.-G. Stammler, B. Neumann, R. A. Harder, L. Weber, M. A. Fox, *Angew. Chem. Int. Ed.* **2014**, *126*, 3702−3705.

59. L. Weber, J. Kahlert, L. Bohling, A. Brockhinke, H.-G. Stammler, B. Neumann, R. A. Harder, P. J. Low, M. A. Fox, *Dalton Trans.* **2013**, *42*, 2266−2281.

60. K.-R. Wee, Y.-J. Cho, J. K. Song, S. O. Kang, *Angew. Chem. Int. Ed*. **2013**, *52*, 9682−9685.

61. H. Mori, K. Nishino, K. Wada, Y. Morisaki, K. Tanaka, Y. Chujo, *Mater. Chem. Front*. **2018**, *2*, DOI: 10.1039/C7QM00486A.

62. K. Nishino, K. Uemura, K. Tanaka, Y. Chujo, *New J. Chem*. **2018**, *16*, DOI: 10.1039/c7nj04283c.

63. K. Nishino, K. Uemura, K. Tanaka, Y. Morisaki, Y. Chujo, *Eur. J. Org. Chem*. **2018**, *2018*, DOI: 10.1002/ejoc.201701641.

Figures and Tables

Scheme 1. Thermally-induced rearrangement in *o*-carborane

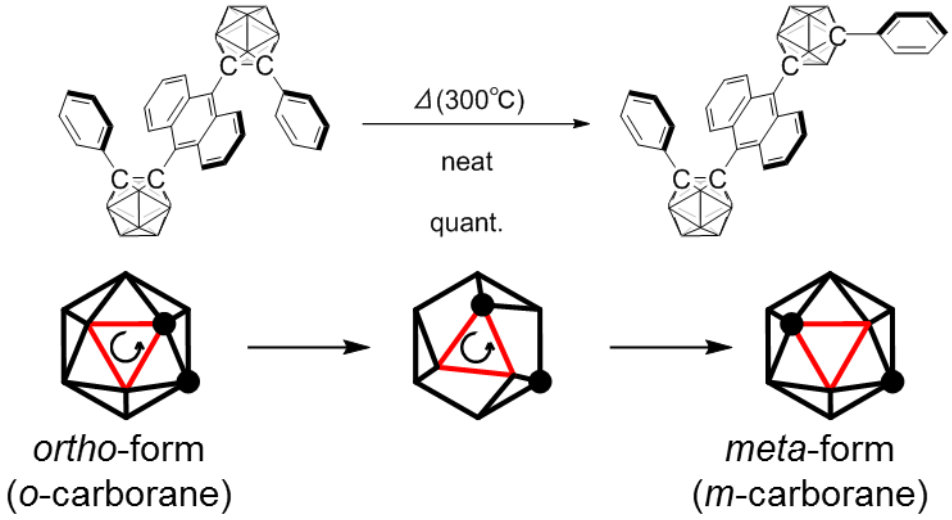

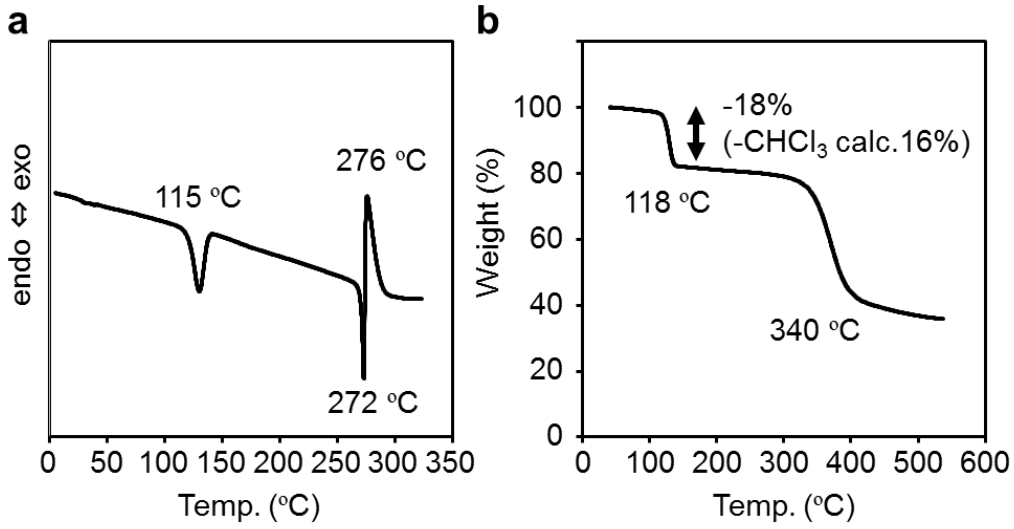

Figure 1. (a) DSC thermogram and (b) TGA curve of **1**·$CHCl_3$ at heating rate of 10 °C/min under N_2 atmosphere.

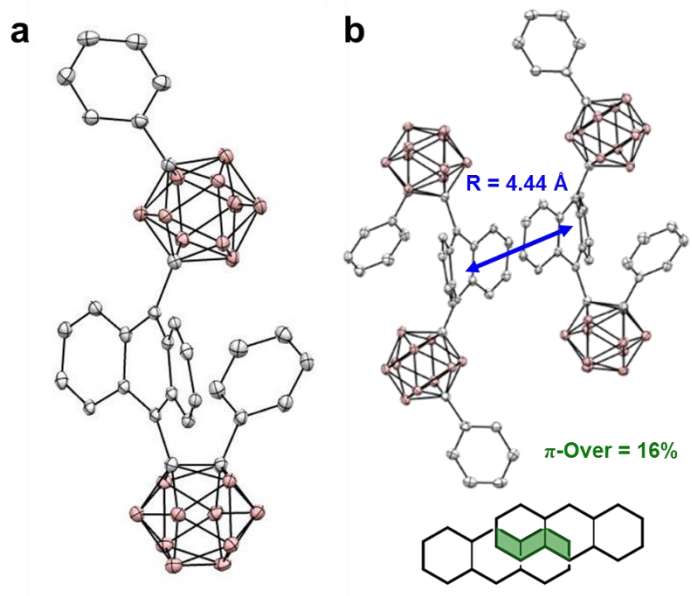

Figure 2. (a) Molecular structure and (b) π-dimer formation of **2** determined by X-ray crystallography.

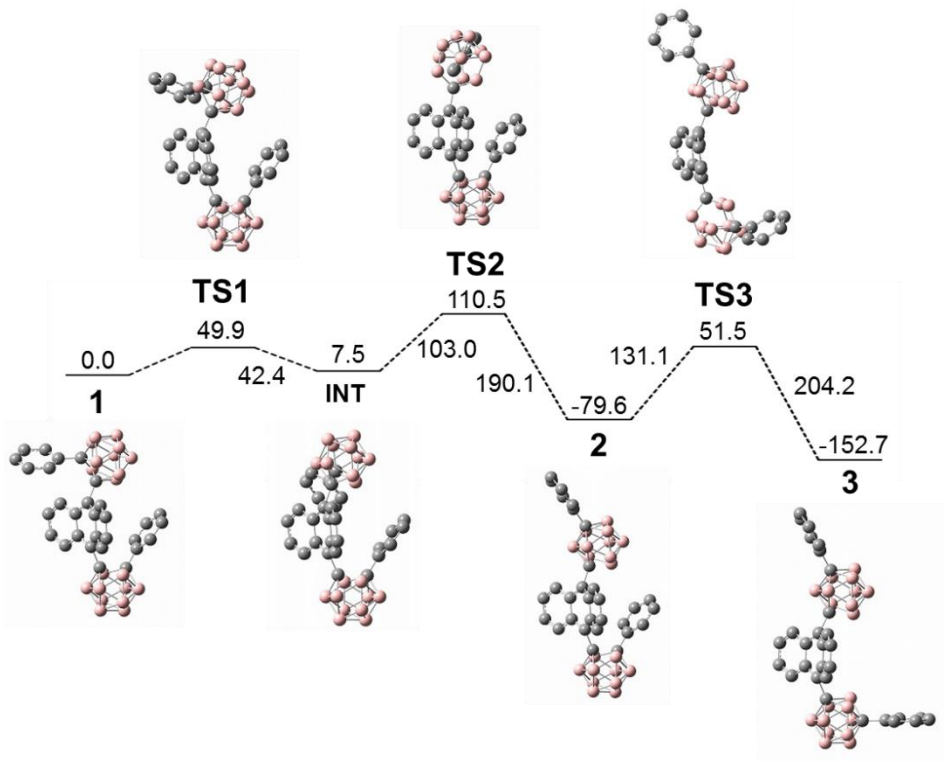

Figure 3. Calculated relative free energies and geometries of **1**.

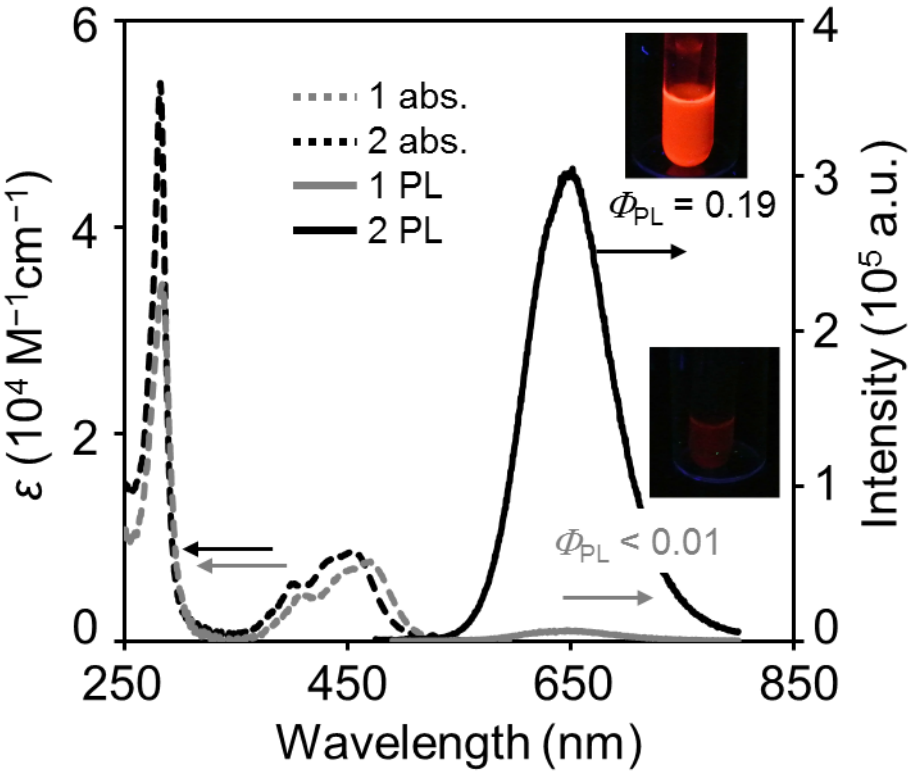

Figure 4. UV−vis absorption and PL spectra of **1** and **2** in THF solutions (1.0×10^{-5} M). Excitation wavelengths were at $\lambda_{abs,max}$. Pictures were taken under UV irradiation (365 nm).

Table 1. Optical properties of the modified acenes before and after heating[a]

	λ_{PL} [nm]			Φ_{PL}[e]		
	THF[b]	aggregation[c]	crystal	THF[b]	aggregation[c]	crystal
1	647	643	628[d]	<0.01	0.08	0.77[d]
2	652	642	632	0.19	0.38	0.59
Tetracene[f]	–	759	742	–	0.01	<0.01
After heating[g]	568	657	670	0.30	0.07	0.07

[a]Excited at each $\lambda_{abs,max}$. [b]1.0×10^{-5} M at room temperature. [c]1.0×10^{-5} M in THF : H_2O = 1 : 99 at room temperature. [d]The data were collected from the chloroform incorporated crystal (**1**·$CHCl_3$). [e]Determined as an absolute value with the integration sphere method. [f]Ref. 46. [g]Product from the tetracene derivative after heating at 300 °C for 10 min.

Graphical Abstract

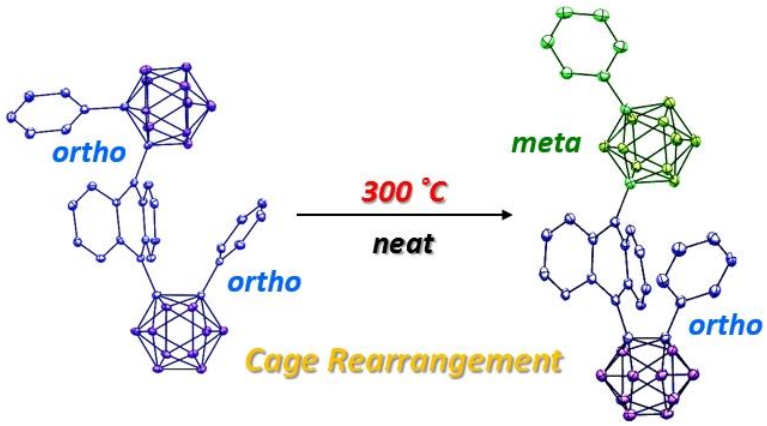

The thermal reaction of the bis-*o*-carborane-modified anthracene was detected. It was proved that thermal rearrangement from *ortho*- to *meta*-carborane occurred. From optical measurements, not only luminescent efficiencies but also aggregation-induced emission enhancement were observed. It was also demonstrated that this reaction was applicable with the tetracene molecule to obtain the deep-red luminescent dye.

A key topic: Luminescent carborane